American Journal of Mechanical Engineering, 2015, Vol. 3, No. 3A, 22-26
Available online at http://pubs.sciepub.com/ajme/3/3A/4

DOI:10.12691/ajme-3-3A-4

Experimental Validation of Numerical Results of a Göttingen 188 Airfoil Wind Turbine for a 40 ° Blade Angle

Zied Driss[1,*], Tarek Chelbi[1], Ahmed Kaffel[2], Mohamed Salah Abid[1]

[1]Laboratory of Electro-Mechanic Systems (LASEM), National School of Engineers of Sfax (ENIS), University of Sfax (US), B.P. 1173, Road Soukra, km 3.5, 3038 Sfax, TUNISIA
[2]University of Maryland College Park, MD 20742, USA
*Corresponding author: Zied.Driss@enis.rnu.tn

Received May 20, 2015; Revised June 22, 2015; Accepted July 14, 2015

Abstract In this paper, an experimental validation of numerical results of a Göttingen 188 airfoil wind turbine has been achieved. For thus, a detailed description of the used wind tunnel and the various manipulations performed with the mentioned turbine are presented. The experimental setup was developed to estimate the velocity profiles and the static torque for a wedging angle of the blade equal to β=40°. In these conditions, we have proved that the static torque presents the maximum value compared with the others tested wedging angles. Our goal is to characterize the aerodynamic structure and to validate the numerical results developed using Computational Fluid Dynamic (CFD) code.

Keywords: *experimental validation, wind tunnel, wind turbine, Göttingen 188 airfoil, wedging angle*

Cite This Article: Zied Driss, Tarek Chelbi, Ahmed Kaffel, and Mohamed Salah Abid, "Experimental Validation of Numerical Results of a Göttingen 188 Airfoil Wind Turbine for a 40 ° Blade Angle." *American Journal of Mechanical Engineering*, vol. 3, no. 3A (2015): 22-26. doi: 10.12691/ajme-3-3A-4.

1. Introduction

Facing economic problems due to large increases in fuel prices, the world has moved towards the exploitation of new and renewable energies. These are inexhaustible and inexpensive compared to the energies of noble viewpoint of electric power generation. The steps to prepare a truly sustainable development are to increase the share of renewable resources for electricity generation. In this context, the production of electricity by wind turbines is playing a major role. In this context, a lot of scientists have experimentally and numerically examined the effects of such parameter design as blades number and airfoil profile. For example, Leifsson and Koziel [1] presented a transonic airfoil design optimization methodology that uses a computationally cheap, physics-based low-fidelity model to construct a surrogate of an accurate but CPU intensive high-fidelity model. Strinath and Mittal [2] utilized a continuous adjoint method for the design of airfoils in unsteady viscous flows for α=4° and Re=104. A stabilized finite element method based on the SUPG/PSPG stabilizations has been used to solve, both, flow and adjoint equations. The results of an experimental investigation of the heat transfer coefficients for forced convection from a NACA-63421 airfoil are presented by Wang et al. [3]. Wind tunnel measurements of convection coefficients are obtained for air flow temperatures from 20 to 30 ℃. The experimental data are correlated with respect to the Nusselt and Reynolds numbers. Henriques et al. [4] showed that a pressure-load inverse design method was successfully applied to the design of a high-loaded airfoil for application in a small wind turbine for urban environment. Predescu et al. [5] described the experimental work in a wind tunnel on wind turbine rotors having different number of blades and different twist angle. The aim of the work is to study the effects of the number of blades, the blade tip angles and twist angle of the blades on the power coefficient of the rotor. Also, the experiments evaluate to what extent the power coefficient of the turbine rotor depends on the operating wind speed. Sicot et al. [6] investigated the aerodynamic properties of a wind turbine airfoil. Particularly, they studied the influence of the inflow turbulence level (from 4.5% to 12%) and of the rotation on the stall mechanisms in the blade. A local approach was used to study the influence of these parameters on the separation point position on the suction surface of the airfoil, through simultaneous surface pressure measurements around the airfoil. Schreck and Robinson [7] showed that wind turbine blade aerodynamic phenomena can be broadly categorized according to the operating state of the machine, and two particular aerodynamic phenomena assume crucial importance. At zero and low rotor yaw angles, rotational augmentation determines blade aerodynamic response. At moderate to high yaw angles, dynamic stall dominates blade aerodynamic. Hu et al. [8] showed that Coriolis and centrifugal forces play important roles in 3D stall-delay. At the root area of the blade, where the high angles of

attack occur, the effect of the Coriolis and centrifugal forces is strong. Thus, it shows apparent stall-delay phenomenon at the inner part of the blade. However, by increasing the Reynolds number, the separation position has a stronger effect than by increasing the Coriolis and centrifugal forces. Wright and Wood [9] showed that the acceleration and deceleration of the rotor at speeds below its controlled maximum speed, and for a range of wind speeds was calculated and compared with data. Excellent agreement was found. Hirahara et al. [10] showed that a unique and very small wind turbine, mF500 with 500 mm diameter and small aspect ratio was developed for wide use in urban space. The basic performance of µF500 was tested for various free stream and load resistance. The airflow around the turbine was investigated by using a particle image velocimetry (PIV). The main goal of the Mirzaei et al. [11] investigation was to understand the flow field structure of the separation bubble formed on NLF-0414 airfoil with glaze-ice accretions using CFD and hot-wire anemometry and comparing these results with previous researches performed on NACA 0012 airfoil.

In this paper, we are interested on the study of a Göttingen 188 airfoil wind turbine. Particularly, a detailed description of the used wind tunnel and the various manipulations performed will be presented to achieve an experimental validation of numerical results.

2. Materials and Method

2.1. Wind Turbine

The present work focuses on the horizontal axis wind turbine. The wind turbine is constituted of three adjustable blades of the Göttingen 188 airfoil. In this application, the airfoil is characterised by a blade length equal to l=100 mm and a chord length equal to C=43 mm. The radius rotor is equal to R=157 mm (Figure 1). Indeed, the wind turbine is equipped by a system to change the wedging angle β, measured between the blade rotation plane and the chorde. The experimental investigation has been developed using wind tunnel. The wind turbine has been introduced through a hole situated on the top of the test vein. Particularly, a vertical axis is used to maintain the rotor. This installation permits to study the effect of the wedging angle and the Reynolds number on the global characteristics of the wind turbine (Figure 2).

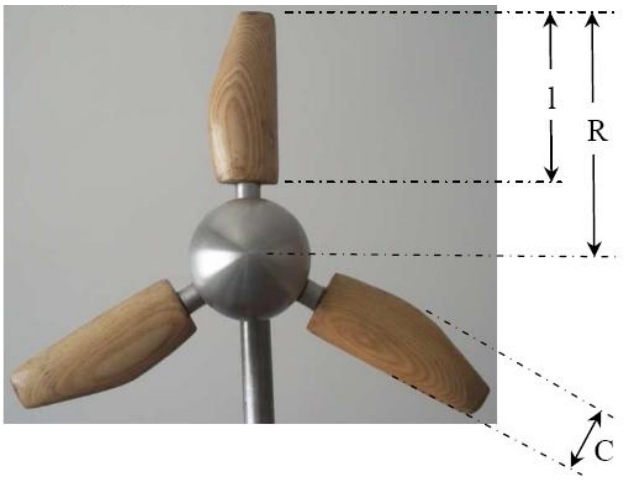

Figure 1. Göttingen 188 airfoil wind turbine

2.2. Measuring Instruments

To initiate the various processes necessary for the characterization of the rotor with the wind tunnel, several measuring instruments were used. Among which include the tachometer, the anemometer, the static torque meter and the dynamometer. The experimental study conducted as part of this work involved the realisation of a horizontal axis wind turbine, a wind tunnel. Experimental trials, allowing the determination of the static torque M_s, the dynamic torque Md and the velocities profiles in different directions pre-selected in the test section. Such a system is equipped with a specific instrument for the development of various experimental tests required at the laboratory scale. The anemometer measures wind speed in different positions in the pre-selected test section or outside (Figure 2). This is feasible, since the range of variation of speed is between 0.2 and 20 $m.s^{-1}$ with a resolution which reaches 0.1 $m.s^{-1}$. The different characteristics of the used anemometer are summarized in Table 1.

Figure 3 presents the static torque meter used for measuring the static torque exerted by the rotor. Under these conditions, the wind turbine is held fixed and cannot turn. Therefore, our experience consists on the measure of the aerodynamic force exerted by air on the wings at different angular positions. The characteristics of the used torque meter are summarized in Table 2.

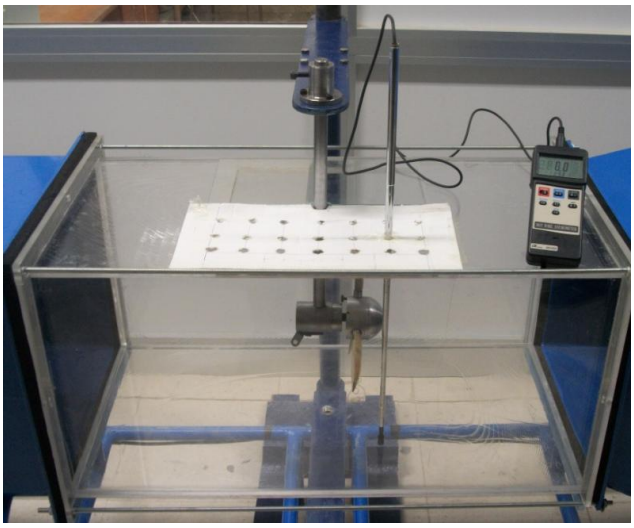

Figure 2. Velocity measuring in the test section

Table 1. Characteristics of the anemometer

Description	Anemometer type AM 4204
Maker	Lutron
Probe type	telescopic
Measurement parameters	Air velocity, temperature, gas flow
Resolution	Air velocity 0.1 $m.s^{-1}$ Temperature 0.1 ℃
Precision	Air velocity 5% Temperature ±0,8 ℃
Measuring range	Velocity 0.1 m.s-1 Temperature from -20 ℃ to +70 ℃

Figure 3. Torque meter measuring

Table 2. Characteristics of the torque meter

Description	Static torque meter TQ 8800
Maker	Lutron
Measurement parameters	Static torque
Measurement range	Max 0-147.1 N.cm
Resolution	0,1 N.cm
Precision	± (1.5 % + 5d)
Overload capacity	220.1 N.cm max
Dimension	180 x 72 x 32 mm

3. Results and Discussion

In this study, we chose to study the flow regime defined by the Reynolds number equal to Re=265403 and for a wedging angle equal to β=40°.

3.1. Profiles of the Magnitude Velocity

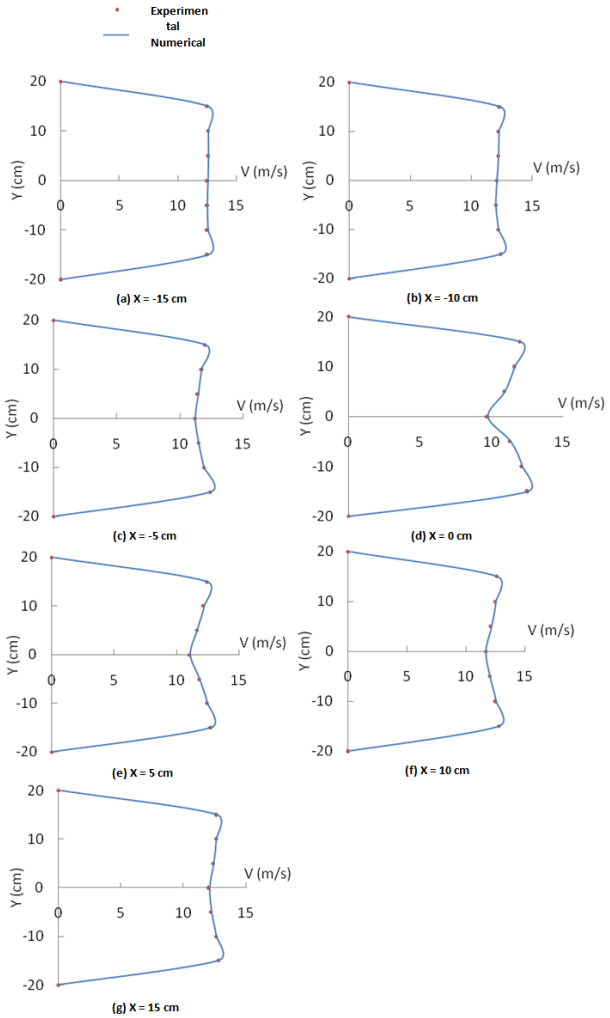

Figure 4. Profiles of the magnitude velocity in the plane z=-15 cm

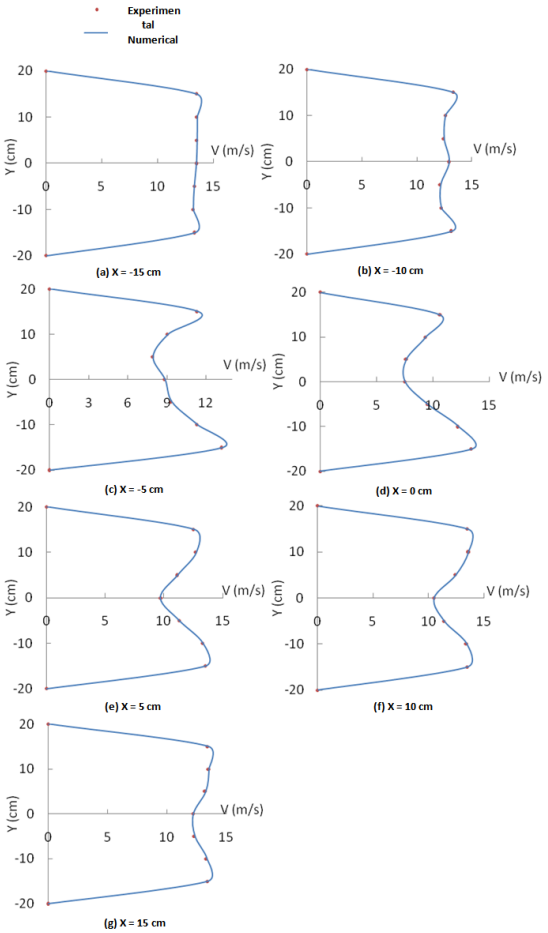

Figure 5. Profiles of the magnitude velocity in the plane z=0 cm

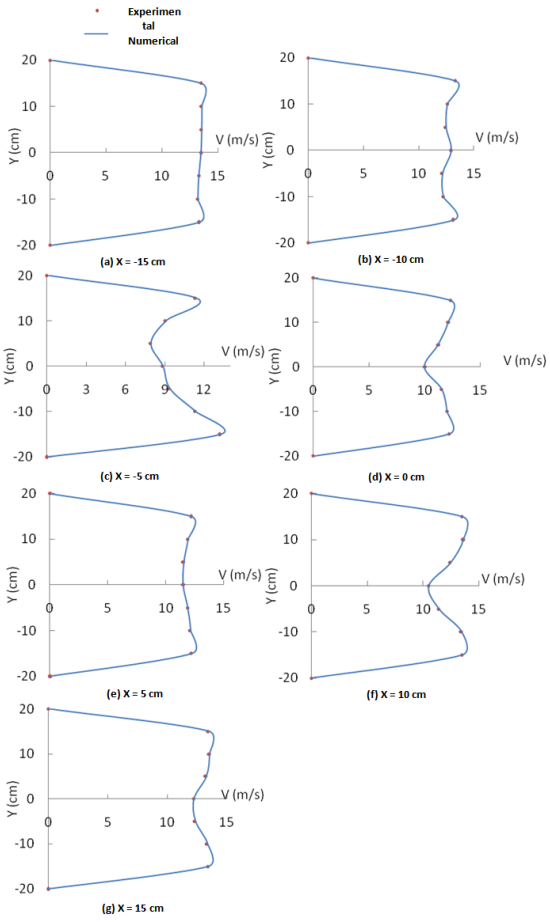

Figure 6. Profiles of the magnititude velocity in the plane z=15 cm

Figure 4, Figure 5 and Figure 6 show the velocity profiles in the transverse plane defined by the axial positions equals to z=-15 cm, z=0 cm and z=15 cm respectively. These planes are placed in the test vein of the wind tunnel in the downstream, the blade plane and the upstream of the wind turbine. Each of these profiles are situated on the directions defined by X=-15 cm, X=-10 cm, X=-5 cm, X=0 cm, X=5 cm, X=10 cm and X=15 cm. By setting the two directions X and Z, the work is reduced to a measure the magnitude velocity at different altitudes Y. This is measured after positioning of the anemometer in the correct position and reading the value displayed on the screen. According to these results, it has been noted that far from the wind turbine, the value of speed is almost constant over the entire length of the test section. It was only at the walls that the velocity is zero. By approaching to the wind turbine, the magnitude velocity profiles undergo some oscillating indicating that the speed is no longer uniform. On the meeting of the wind turbine blades, the magnitude velocity is very weak. Moreover, there is a slight increase in average velocity in the wind turbine downstream. In these conditions, the maximum value of the magnitude velocity reaches V=13.5 m.s^{-1}.

3.2. Contours plots of the magnitude velocity

Figure 7 and Figure 8 show the velocity profiles in the transverse plane defined by the axial positions equals to z=-15 cm and z=15 cm respectively. These planes are placed in the test vein of the wind tunnel in the downstream and the upstream of the wind turbine. According to these results, it's clear that the distribution of the magnitude velocity is uniform inside the test vein in the upstream of the wind turbine. However, it decreases until V=7 m.s^{-1} in the downstream after crossing the wind turbine. Indeed, the magnitude velocity decreases near the wall and becomes null at his meeting.

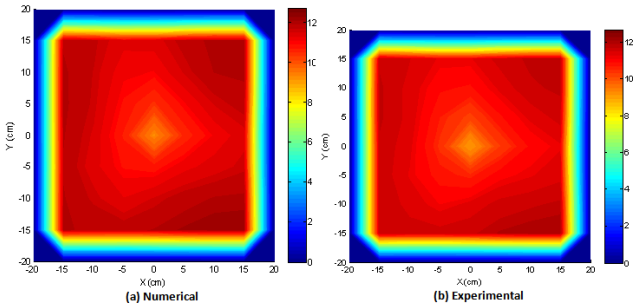

Figure 7. Distribution of the magnititude velocity in the plane z=-15 cm

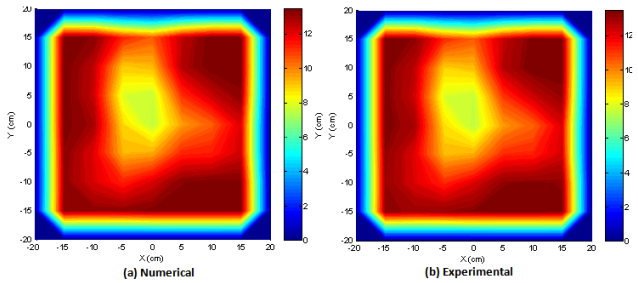

Figure 8. Distribution of the magnititude velocity in the plane z=15 cm

3.3. Static Torque

Figure 9 presents the variation of the static torque M_s for different wedging angles β. In this work, the static torque is measured using the torque meter types TQ 8800 mounted directly on the rotor axis. These results relate well to the study of the influence of the wedging angle on the static torque. According to these results, it has been noted that this curve has a parabolic shape.

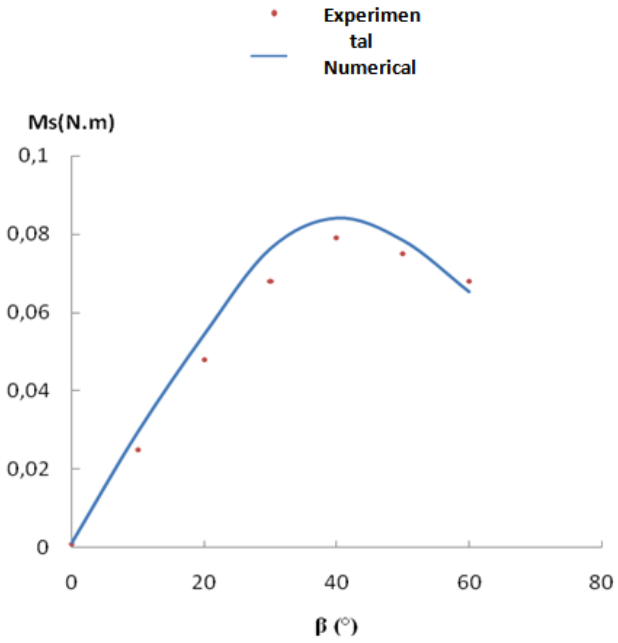

Figure 9. Variation of the static torque

With the increase of the wedging angle β, the value of the static torque increases and reaches a maximum and then it decreases. Indeed, it has been noted that the maximum static torque M_s is obtained for a wedging angle equal to β=40°. In this case, the value of the static torque is equal to M_s=0.082 N.m.

4. Conclusions

In this paper, we have achieved an experimental validation of numerical results of a Göttingen 188 airfoil wind turbine for a 40 ° blade angle. For thus, we have presented a detailed description of the used wind tunnel and the considered manipulations. Particularly, we are interested on the measuring of the average velocity of the flow in different positions of the test vein. The static torque measurements are also performed for different wedging angles of the blade. In the future, we propose to study others geometrical parameters.

References

[1] L. Leifsson, S. Koziel, Multi-fidelity design optimization of transonic airfoils using physics-based surrogate modeling and shape-preserving response prediction, Journal of Computational Science 1 (2010) 98-106.

[2] D.N. Srinath, S. Mittal, Optimal aerodynamic design of airfoils in unsteady viscous flows, Computer Methods in Applied Mechanics and Engineering 199 (2010) 1976-1991.

[3] X. Wang, E. Bibeau, G.F. Naterer, Experimental correlation of forced convection heat transfer from a NACA airfoil, Experimental Thermal and Fluid Science 31 (2007) 1073-1082.

[4] J.C.C. Henriques, F. Marques da Silva, A.I. Estanqueiro, L.M.C. Gato, Design of a new urban wind turbine airfoil using a pressure-load inverse method, Renewable Energy 34 (2009) 2728-2734.

[5] M. Predescu, A.Bejinariu, O.Mitroi, A. Nedelcu, Influence of the Number of Blades on the Mechanical Power Curve of Wind Turbines, International Conference on Renewable Energies and Power Quality (2009).

[6] C. Sicot, P. Devinant, S. Loyer, J. Hureau, Rotational and turbulence effects on a wind turbine blade. Investigation of the stall mechanisms, Journal of Wind Engineering and Industrial Aerodynamics 96 (2008) 1320-1331.

[7] S.J. Schreck and M.C. Robinson, Horizontal Axis Wind Turbine Blade Aerodynamics in Experiments and Modeling, IEEE Transactions on Energy Conversion, 22 (2007) 61-70.

[8] D. Hu, O. Hua, Z. Du, A study on stall-delay for horizontal axis wind turbine, Renewable Energy 31 (2006) 821-836.

[9] A.K. Wrigh, D.H. Wood, The starting and low wind speed behaviour of a small horizontal axis wind turbine, Journal of Wind Engineering and Industrial Aerodynamics 92 (2004) 1265-1279.

[10] H. Hirahara, M. Zakir Hossain, M. Kawahashia, Y. Nonomura, Testing basic performance of a very small wind turbine designed for multi-purposes, Renewable Energy 30 (2005) 1279-1297.

[11] M. Mirzaei, M.A. Ardekani, M. Doosttalab, Numerical and experimental study of flow field characteristics of an iced airfoil, Aerospace Science and Technology, 13 (2009) 267-27.

[12] Damak A, Driss Z, Abid MS. Experimental investigation of helical Savonius rotor with a twist of 180 °, Renewable Energy 52 (2013) 136-142.